

1 **Investigating the dynamics of recombinant protein secretion from a microalgal host**

2

3 **Author names and affiliations:** Kyle J. Lauersen¹, Isabel Huber¹, Julian Wichmann¹,
4 Thomas Baier¹, Andreas Leiter³, Volker Gaukel³, Viktor Kartushin², Anke Rattenholl²,
5 Christian Steinweg⁴, Lena von Riesen⁴, Clemens Posten⁴, Frank Gudermann², Dirk
6 Lütkemeyer², Jan H. Mussnug¹, and Olaf Kruse^{1,*}

7

8 ¹Bielefeld University, Faculty of Biology, Center for Biotechnology (CeBiTec),
9 Universitätsstrasse 27, 33615, Bielefeld, Germany.

10 ²Institute of Biotechnological Process Engineering, Faculty of Engineering and
11 Mathematics, University of Applied Sciences, Universitätsstrasse 27, 33615 Bielefeld,
12 Germany.

13 ³Karlsruhe Institute of Technology (KIT), Institute of Process Engineering in Life
14 Sciences, Section I: Food Process Engineering, Kaiserstraße 12, 76131 Karlsruhe,
15 Germany.

16 ⁴Karlsruhe Institute of Technology (KIT), Institute of Process Engineering in Life
17 Sciences, Section III: Bioprocess Engineering, Fritz-Haber-Weg 2, 76131 Karlsruhe,
18 Germany.

19

20 ***Corresponding Author:** Olaf Kruse, olaf.kruse@uni-bielefeld.de

21 **Present/Permanent address:** Bielefeld University, Faculty of Biology, Center for
22 Biotechnology (CeBiTec), Universitätsstrasse 27, 33615 Bielefeld, Germany.

23 Phone: +49 521 106-12258, Fax: +49 521 106-12290

24

25 **Author contributions**

- 26 • Kyle Lauersen was responsible for manuscript writing, figure design, collaboration
27 organization, the development of strain UVcCA, secreted protein preparation for ice
28 recrystallization analysis, bioluminescence analysis in the laboratory of Frank
29 Gudermann and Dirk Lütkemeyer, as well as dot-blotting.
30
- 31 • Isabel Huber and Julian Wichmann were responsible for cultivation and media
32 screening experiments as well as culture parameter data collection.
33
- 34 • Thomas Baier was responsible for cloning and transformation of pOpt_cCA_gLuc_Paro
35 and pOpt_cCA_gLuc_LpIBP_Paro vectors into strain UVM4.
36
- 37 • Andreas Leiter and Volker Gaukel were responsible for ice recrystallization inhibition
38 analysis.
39
- 40 • Viktor Kartushin, Anke Rattenholl, Frank Gudermann, and Dirk Lütkemeyer were
41 responsible for wave-bag cultivation of strain UVcCA and daily sample collection /
42 experimental organization.
43
- 44 • Christian Steinweg, Lena von Riesen, and Clemens Posten were responsible for the
45 cultivation of strain UVcCA and daily culture parameter sampling of the flat-panel
46 photobioreactor cultivation.
47
- 48 • Jan Mussgnug was involved in manuscript preparation and writing as well as
49 experimental design.
50
- 51 • Work by Kyle Lauersen was conducted in the laboratory of Prof. Dr. Olaf Kruse, who
52 was involved in experimental design and manuscript preparations.
53

54 **Abstract**

55 Production of recombinant proteins with microalgae represents an alternative platform
56 over plant or bacterial based expression systems for certain target proteins. Secretion of
57 recombinant proteins allows accumulation of the target product physically separate from
58 the valuable algal biomass. To date, there has been little investigation into the dynamics of
59 recombinant protein secretion from microalgal hosts - the culture parameters that
60 encourage secreted product accumulation and stability, while encouraging biomass
61 production. In this work, the efficiency of recombinant protein production was optimized
62 by adjusting cultivation parameters for a strain of *Chlamydomonas reinhardtii* previously
63 engineered to secrete a functional recombinant *Lolium perenne* ice binding protein
64 (*LpIBP*), which has applications as a frozen food texturing and cryopreservation additive,
65 into its culture medium. Three media and several cultivation styles were investigated for
66 effects on secreted *LpIBP* titres and culture growth. A combination of acetate and carbon
67 dioxide feeding with illumination resulted in the highest overall biomass and recombinant
68 protein titres up to 10 mg L⁻¹ in the culture medium. Purely photoautotrophic production
69 was possible using two media types, with recombinant protein accumulation in all
70 cultivations correlating to culture cell density. Two different cultivation systems were used
71 for scale-up to 10 litre cultivations, one of which produced yields of secreted recombinant
72 protein up to 12 mg L⁻¹ within six cultivation days. Functional ice recrystallization
73 inhibition (IRI) of the *LpIBP* from total concentrated extracellular protein extracts was
74 demonstrated in a sucrose solution used as a simplified ice cream model. IRI lasted up to
75 seven days, demonstrating the potential of secreted products from microalgae for use as
76 food additives.

77

78 **Keywords:** Microalgae, *Lolium perenne* ice-binding protein, recombinant protein
79 secretion, Flat panel photobioreactor, Wave bag culture, *Chlamydomonas reinhardtii*.

80

81 **Abbreviations:**

82 *gLuc* – *Gaussia princeps* luciferase

83 *cCA* – secretion signal of *C. reinhardtii* carbonic anhydrase 1

84 IRI – ice recrystallization inhibition

85 *LpIBP* – *Lolium perenne* ice binding protein

86 HiT – High-Tris media

87 **1. Introduction**

88 The Chlorophyte microalgae *Chlamydomonas reinhardtii* has served as a valuable model
89 organism for fundamental photosynthetic and biological analysis for many years (Rochaix
90 1995). Currently this alga has the most well developed molecular toolkit of any eukaryotic
91 microalgae, and transformation of nuclear, chloroplast, and mitochondrial genomes is
92 possible (Bateman and Purton 2000; Kindle 1990; Remacle et al. 2006). Chloroplast based
93 recombinant protein (RP) expression in this organism has been shown to achieve titres up
94 to 21% total soluble protein (TSP) (Surzycki et al. 2009). This capacity, in addition to the
95 generally regarded as safe (GRAS) status of *C. reinhardtii*, has led to its proposed use for
96 molecular farming of high value RPs, both as purified products, and as whole-cell edible
97 gut-active therapeutics (Franklin and Mayfield 2004; Rasala and Mayfield 2014; Rosales-
98 Mendoza et al. 2012).

99 In contrast, nuclear transgene expression has resulted in significantly lower titres of RP,
100 with a maximum reported of 0.25% TSP (Lauersen et al. 2015; Rasala et al. 2013; Rasala
101 et al. 2012). Nuclear transgene expression is mediated by eukaryotic translational
102 machinery, and is inherently more regulated than its plastid counterparts (Mayfield et al.
103 2007; Rasala and Mayfield 2014). However, nuclear based gene expression presents the
104 possibility of subcellular targeting of RPs to various cellular compartments,
105 posttranslational modifications, and the capacity for secretion of RPs into culture medium
106 (Lauersen et al. 2013a; Lauersen et al. 2013b; Rasala et al. 2012).

107 The capacity of microalgae for growth driven by photosynthesis presents potentially
108 sustainable production through these hosts, using only water, (sun)light energy and carbon
109 dioxide as inputs (Wijffels et al. 2013). However, to date, technical limitations in large-
110 scale photosynthetic algal cultivation prevent the widespread use of these organisms for
111 many industrial concepts. Indeed, the first publication of greenhouse-style cultivation of
112 transgenic *C. reinhardtii*, which expressed a target edible therapeutic in the chloroplast,
113 was published only recently (Gimpel et al. 2014).

114 In light of the difficulties of engineering algal production systems, secretion of
115 recombinant products from the algal host presents the potential for a new layer of
116 production value for algal cultivation concepts, allowing the recombinant product to be
117 harvested independently of the valuable algal biomass. Although therapeutic RPs have
118 dominated research in *C. reinhardtii* transgenics, two examples of industrially relevant RP
119 production have been demonstrated via expression from the nuclear genome and secretion
120 into culture medium: a xylanase (Rasala et al. 2012), and recently in our laboratory, an

121 active ice binding protein (IBP) (also known as ice structuring, antifreeze, or IRI protein)
122 from the perennial ryegrass *Lolium perenne* (*LpIBP*) with *C. reinhardtii* (Lauersen et al.
123 2013b). The latter was accomplished as a fusion protein made from a codon optimized
124 *Gaussia princeps* luciferase (*gLuc*) gene, synthetically modified to contain a *C. reinhardtii*
125 carbonic anhydrase secretion signal (*cCA*), which allowed rapid identification of
126 transformants exhibiting robust expression and secretion of the *gLucLpIBP* fusion
127 (Lauersen et al. 2013a; Lauersen et al. 2013b).

128 The *LpIBP* limits the thermodynamically favoured growth of ice crystals at high sub-zero
129 temperatures, a phenomenon known as ice recrystallization (IR), which this protein
130 controls in its native plant to assist overwintering (Lauersen et al. 2011; Middleton et al.
131 2009; Yu et al. 2010). However, IR is also a common cause of frozen food spoilage, the
132 most pertinent example of IR is the unpleasant texture of ice cream stored for long periods
133 (Donhowe and Hartel 1996a; Donhowe and Hartel 1996b). Given the robust IRI activity of
134 the *LpIBP*, it has been proposed for use as a frozen food additive to limit frost damage over
135 increased storage time (Griffith and Ewart 1995; Hassas-Roudsari and Goff 2012).

136 In both published examples of industrially relevant RP secretion from *C. reinhardtii*, only
137 minimal efforts to investigate the culture parameters for stable protein production via
138 secretion from the algal system were conducted (Lauersen et al. 2013b; Rasala et al. 2012).
139 However, secreted RPs pose additional challenges for scale-up of cultivation systems, as
140 the stability requirements of proteins in the culture medium may be different than those of
141 the expression host. Therefore, we investigated culture parameters which would allow and
142 optimize the efficiency of concomitant biomass and secreted RP production from *C.*
143 *reinhardtii* using the *gLucLpIBP* as a model secreted RP. Different culture media as well
144 as growth regimes were investigated, and production up to 10 L scale was compared for
145 two selected culture systems.

146

147

148 2. Materials and Methods

149 2.1 Cultivation conditions, plasmids, transformation, and screening of transgenic

150 *C. reinhardtii*

151 All precultures in this work were grown in TAP medium (Gorman and Levine 1965) under
152 standard conditions with $\sim 150 \mu\text{mol photons m}^{-2}\text{s}^{-1}$ on a standard rotary shaker. UVM4
153 (graciously provided by Prof. Dr. Ralph Bock) and the *gLucLpIBP* secretion strain
154 UVcCA (Lauersen et al. 2013a) cultures were routinely grown in TAP medium with
155 $150 \mu\text{mol photons m}^{-2}\text{s}^{-1}$ light intensity in shake flasks or on TAP(agar) plates.
156 *C. reinhardtii* UVM4 is a ultraviolet light derived mutant of CC-4350 (cw15 arg7-8 mt+
157 [Matagne 302]) which was transformed with the emetine resistance cassette CRY1 as well
158 as the ARG7 argininosuccinate lyase complementation vector and subsequently
159 demonstrated nuclear transgene expression with high efficiency (Neupert et al. 2009). CC-
160 4350 is available from the Chlamydomonas Resource Center ([http://](http://chlamycollection.org)
161 chlamycollection.org).

162 UVM4 was transformed with plasmid pOpt_cCA_gLuc_Paro (Lauersen et al. 2015), and a
163 variation which has the codon optimized *Lolium perenne* ice binding protein (NCBI
164 Access. No.: KF475785) cloned between *EcoRV* and *EcoRI* sites as a C-terminal fusion to
165 the *gLuc* as was originally demonstrated for the pcCAG*gLucLpIBP* vector (Lauersen et al.
166 2013a; Lauersen et al. 2013b). Transformations were performed with glass bead agitation
167 as previously described (Kindle 1990). Transformants were recovered on TAP(agar) plates
168 containing paromomycin at 10 mg L^{-1} with $150 \mu\text{mol photons m}^{-2}\text{s}^{-1}$ light intensity, and
169 maintained on TAP(agar) plates by colony stamping.

170 Mutants were screened in the same way in which UVcCA was originally isolated, using
171 plate-level bioluminescence assays as previously described (Lauersen et al. 2013a) from a
172 population of 480 mutants (5x96 colony plates) per construct. Four mutants exhibiting the
173 most robust bioluminescence signal from each vector construct were selected for
174 cultivation in liquid culture. The relative bioluminescence of culture medium resulting
175 from secretion of either the *gLuc* alone or *gLucLpIBP*, in late logarithmic phase was
176 assessed in a Tecan infinite M200 plate reader (Männedorf, Switzerland) using black
177 microtitre plates. Analysis of bioluminescence signal was conducted immediately after
178 addition of 0.01 mM coelenterazine (PJK shop) with 2000 ms integration time and
179 normalised to cell density. Measurements were conducted in technical triplicate, from three
180 biological cultivation replicates.

181 **2.2 Investigations of culture pre-conditions for *gLucLpIBP* secretion and UVcCA** 182 **growth**

183 For all media investigations, precultures were centrifuged for 3 min at 1000xg followed by
184 resuspension with target medium, this step was repeated two times in order to remove
185 unwanted residual medium components from the cells.

186 Three styles of cultivation at the 1 L scale were investigated, UVcCA was grown in TAP
187 medium without gassing in shake, baffled shake, or stirred 1 L volumes at
188 $\sim 200 \mu\text{mol photons m}^{-2}\text{s}^{-1}$. The relative *gLucLpIBP* secretion from UVcCA in these
189 cultures was analysed by dot-blot of medium samples using the α -*gLuc* antibody with a
190 secreted recombinant *gLuc* produced in *Kluyveromyces lactis* as standard (available
191 commercially from Avidity) as previously described (Lauersen et al. 2013a).

192 **2.3 Comparisons of media and cultivation strategies for the secreted *gLucLpIBP***

193 TAP medium was used to cultivate strain UVcCA heterotrophically (acetate, dark, air
194 bubbling) and photo-mixotrophically with low (acetate, light, air bubbling) or high CO₂
195 (acetate, light, 3% CO₂ bubbling) levels. Strict photoautotrophic cultivation (3% CO₂) and
196 RP production dynamics were investigated in Sueoka's high salt medium (HSM) (Sueoka
197 1960), and an in-house 'High-Tris' medium (designated HiT) containing 12 g L⁻¹ Tris (for
198 recipe see Table S1). All cultivations were conducted in three biological replicates of
199 400 mL stirred glass flasks, bubbled with either air or air plus 3% CO₂ at 50 L h⁻¹ and
200 $350 \mu\text{mol photons m}^{-2}\text{s}^{-1}$, unless cultivated in the dark. Culture parameters including cell
201 density and dry biomass were recorded. In addition, daily media samples were taken and
202 bioluminescence readings were performed (not shown) as previously described (Lauersen
203 et al. 2013a). Absence of bacterial contamination was controlled for by plating culture
204 aliquots on TAP media containing yeast extract, as well as analysis of supernatant clarity
205 following centrifugation. The best performing biological replicate of each cultivation in
206 bioluminescence assays was analysed by dot-blot using the α -*gLuc* antibody as previously
207 described (Lauersen et al. 2013b).

208 **2.4 Cultivation of UVcCA in 10 L flat panel photobioreactor**

209 Cultivation scale-up was conducted with a custom built 10 L flat panel bioreactor using
210 TAP medium. To avoid photoinhibitory effects, illumination was set to
211 $\sim 50 \mu\text{mol photons m}^{-2}\text{s}^{-1}$ for the first day after inoculum and then increased to
212 $\sim 100 \mu\text{mol photons m}^{-2}\text{s}^{-1}$ for the remainder of the cultivation. The culture was inoculated
213 to an initial density of $4 \times 10^6 \text{ cells mL}^{-1}$ from a TAP grown preculture, cultivation was

214 conducted for 144 hours prior to termination. Cultivation temperature was regulated
215 between 27-29 °C with an internal cooling system. Aeration and mixing was accomplished
216 by bubbling with 800 mL min⁻¹ 3% CO₂. The total cultivation volume was ~9 L. Due to
217 formation of foam on top of the culture, approximately 10 mL of antifoam was added to
218 the culture (Antifoam A, Sigma). Formation of sediment was observed which could not be
219 resuspended as an increase of the airflow led to a deformation of the Plexiglas walls. Daily
220 sampling included cell density and dry biomass. Quantification of gLuc in culture medium
221 was conducted as above.

222 **2.5 Cultivation of UVcCA in an illuminated 10 L wave bag bioreactor**

223 The BIOSTAT CultiBag RM system from Sartorius Stedim Biotech GmbH (Göttingen,
224 Germany) was used with a CultiBag RM 20L optical bag (together: Wave bag) for
225 cultivation of UVcCA. The system was set to 13 rocks min⁻¹, at an angle of 8.5° and the
226 process run at room temperature. Cultivation was conducted in TAP medium with 3% CO₂
227 surface aeration and given white light from four fluorescence bulbs in a hanging ballast to
228 between ~150-200 μmol photons m⁻²s⁻¹ depending on the angle of rocking. The bag was
229 filled with 10 L TAP medium through a 0.2 μm sterile filter and inoculated to OD₇₅₀ 0.1
230 from a TAP grown preculture. Cells were counted automatically using the Cedex HiRes
231 System (Roche Diagnostics, Mannheim, Germany) daily in addition to cell dry biomass
232 measurements. Samples were taken daily until termination of cultivation at 144 hours. For
233 quantification of gLuc in culture medium, samples were subjected to dot-blotting as well
234 as bioluminescence analysis as above.

235 **2.6 Simulated food product IRI analysis**

236 IRI activity of secreted gLucLpIBP using total concentrated extracellular protein (CEP)
237 samples from *C. reinhardtii* strain UVcCA was demonstrated in a simplified ice cream
238 model solution (49% sucrose (w/w)). Due to the sugar content water is only frozen partly
239 which leads to the concurrent presence of ice crystals and unfrozen solution during storage.
240 This is a characteristic situation not only for ice cream but for many food and food like
241 systems in which recrystallization occurs. Regand and Goff (2005) used a similar solution
242 with less sucrose (23%) for recrystallization analytics. We decided to use a higher sucrose
243 content because this reveals a more realistic ice content for ice cream as the sucrose
244 represents all solutes in the simplified system and the typical dry mass of ice cream is
245 around 40%. In addition a slightly higher sucrose content simplifies the ice crystal
246 analytics due to the lower ice content during storage without changing the principal RI

247 mechanism (Gaukel et al., 2014). CEP was prepared by cultivation of UVcCA and parental
248 strain UVM4 (WT) in TAP medium bubbled with 3% CO₂ to late logarithmic phase under
249 standard conditions in 10 L stirred flasks with 300 μmol photons m⁻²s⁻¹, followed by
250 centrifugation, microfiltration, and concentration by tangential crossflow filtration of
251 medium as previously described (Lauersen et al. 2013b). IRI activity of *gLucLpIBP* in
252 UVcCA CEP without purification was compared with the activity of equimolar amounts
253 (0.154 μM) of purified fish ice binding protein (also known as antifreeze protein, or ice
254 structuring protein) AFP III, isolated from ocean pout (*Macrozoarces americanus*) (Hew et
255 al. 1984; Hew et al. 1988) (purchased from A/F Protein (Waltham, USA)), and parental
256 strain (WT) total CEP. Sucrose Solutions (49% (w/w)) were prepared with a final
257 concentration of 1 mg L⁻¹ of AFP III, total UVcCA CEP to a final concentration of 5 mg L⁻¹
258 *gLucLpIBP*, and an equivalent concentration of CEP for the parental strain (WT).
259 Ice crystal growth analysis was performed as previously described (Gaukel et al. 2014). An
260 amount of 18 μl of the sample solution was placed between two microscope cover slips on
261 an object slide, then covered with another cover slip and sealed with silicone. Three object
262 slides of each solution were prepared and analysed. The samples were subjected to a fast
263 freezing process by immersion in liquid nitrogen for a few seconds to transform the
264 aqueous solution into a glassy state. After freezing, the samples were stored at a constant
265 temperature of -12 °C, +/- 0.1 °C, in a small storage chamber, placed in a deep-freeze room
266 (also -12 °C). This procedure allows the system to crystallize in a uniform way by heating
267 up from the glassy state. For the principal investigation of the recrystallization mechanism
268 it is a reproducible method for the initial formation of small ice crystals, however, differs
269 from industrial frozen food preparation (Gaukel et al., 2014). The temperature inside the
270 chamber was recorded by a thermocouple during the storage time of 1 week. During
271 storage, pictures of ice crystals were taken at 5 h, 24 h, 49 h, 96 h and 168 h after freezing
272 by a camera (alra SIS20, Olympus, Japan) attached to a polarization microscope (BX41,
273 Olympus, Japan) installed in the deep-freeze room. For evaluation of the pictures, the
274 contours of the ice crystals were manually circumscribed on a computer with the software
275 ImagePro Plus 5.0 (Media Cybernetics, USA). From the defined areas of each crystal, the
276 equivalent diameter was calculated as the diameter of a circle with the same area. 300 to
277 400 ice crystals were analysed from each slide and the mean equivalent diameter was
278 determined. The mean crystal size and standard deviation of the three object slides were
279 then calculated for each sample time point.
280

281 3. Results

282 3.1 Fusion of *LpIBP* to the C-terminus of *Gaussia* Luciferase (*gLuc*) enhances protein 283 secretion efficiency

284 In previous experiments, we demonstrated that the recombinant protein *gLucLpIBP*, a
285 synthetic fusion protein of *Gaussia* Luciferase and *Lolium perenne* ice binding protein,
286 expressed from the *pcCAgLucLpIBP* vector, was secreted from *C. reinhardtii* and
287 accumulated to a maximum of $\sim 10 \text{ mg L}^{-1}$ in standard TAP medium cultivations (Lauersen
288 et al. 2013a; Lauersen et al. 2013b). We were interested to directly compare this with the
289 secretion of *gLuc* alone, as recent analysis of this reporter from the *pOpt_cCA_gLuc_Paro*
290 vector resulted in a maximum expression of only $\sim 0.5 \text{ mg L}^{-1}$ culture under the same
291 conditions (Lauersen et al. 2015). In order to directly compare *gLucLpIBP* secretion to
292 *gLuc*, we constructed a *LpIBP* containing vector, *pOpt_cCA_gLuc_LpIBP_Paro* (Fig. 1A),
293 and transformed this or the vector *pOpt_cCA_gLuc_Paro* into parental strain UVM4.
294 Interestingly, transformants expressing *gLucLpIBP* resulted in higher secreted recombinant
295 protein titres than transformants expressing the *gLuc* marker alone (Fig. 1B) indicating that
296 fusion of *LpIBP* to the C-terminus of *gLuc* resulted in greater secretion into culture
297 medium, although the recombinant protein is of significantly higher molecular weight. The
298 results clearly indicate that molecular factors related to the amino acid sequence must exist
299 which can promote or inhibit recombinant protein production and secretion. Although this
300 is a subject of on-going investigations, these factors currently are not known.

301 3.2 Screening cultivation conditions and media that promote efficient production and 302 secretion of recombinant proteins

303 Mixing of cell cultures is an important factor influencing biomass and recombinant protein
304 production. In our setup, we tested three possible methods, shaking, baffled shaking, or
305 stirring, and compared the respective cell culture growth and secreted recombinant protein
306 production of *gLucLpIBP* in UVcCA medium. As shown in Figure 2, stirred cultures
307 generated significantly higher cell densities in early stages of cultivation, up to 48 h, and
308 exhibited a more rapid accumulation of the secreted *gLucLpIBP* in culture medium (Fig.
309 2A,B). This lead us to use stir-mixed flasks for all further medium investigations,
310 including pre-screening of photoautotrophic cultivations with various in-house medium
311 recipes.

312 Photoautotrophic media screening for growth of UVcCA resulted in the identification of
313 one medium with robust culture performance and secreted *gLucLpIBP* accumulation (see

314 Supporting Information for medium recipe). This medium, called HiT (for High-Tris), was
315 used in subsequent comparative culture performance analysis with common *C. reinhardtii*
316 media (HSM and TAP). Media and growth strategies were then directly compared in
317 standardized triplicate 400 mL batch cultures with the strain UVcCA, and used to
318 determine suitable cultivation styles for the secretion of *gLucLpIBP* into culture media
319 (Fig. 3).

320 Both HSM and HiT media were used to investigate growth under strictly photoautotrophic
321 conditions, with 3%CO₂ bubbling as a sole carbon source and illumination as the energy
322 source. TAP medium was used for investigation of strictly heterotrophic cultivation in the
323 dark with acetate as a sole carbon source, as well as for mixotrophic conditions in the light
324 with either acetate and low (air)- or high (3%)-CO₂ (TAP(air) and TAP(CO₂),
325 respectively). Culture performance was assessed by recording cell density and dry biomass
326 (Fig. 3A, upper and lower panels, respectively) and secreted *gLucLpIBP* titres were
327 quantified by dot-blot of media samples (Fig. 3B). Heterotrophic growth in TAP medium
328 resulted in the lowest performance of all investigated culture set-ups, while mixotrophic
329 cultivation in TAP(CO₂), exhibited the highest performance (Fig. 3A).

330 TAP(CO₂) cultures grew to a cell density of $5.1 \pm 0.25 \times 10^7$ cells mL⁻¹ and a dry biomass of
331 1.33 ± 0.10 g L⁻¹ in 96 hours of cultivation (Fig. 3A). Without the additional CO₂
332 (TAP(air)), the cultures grew to approximately half the cell density and biomass
333 ($2.3 \pm 0.17 \times 10^7$ cells mL⁻¹ and 0.56 ± 0.01 g L⁻¹) in the same period of cultivation time. This
334 result demonstrates that although a reduced carbon source is present in the form of acetate
335 in TAP medium, additional application of CO₂ lead to a significant boost of cell growth.

336 Heterotrophically cultivated cell cultures in the dark (TAP dark) only reached
337 $0.78 \pm 0.2 \times 10^7$ cells mL⁻¹ and 0.19 ± 0.02 g L⁻¹ biomass, indicating that additional light
338 energy was an important factor for optimal cell growth (Fig. 3A). Strictly
339 photoautotrophic cultivation in either HSM or HiT media resulted in cultures with up to
340 $1.4 \pm 0.06 \times 10^7$ cells mL⁻¹ and 1.28 ± 0.10 g L⁻¹, or $2.3 \pm 0.48 \times 10^7$ cells mL⁻¹ and
341 1.13 ± 0.06 g L⁻¹, respectively (Fig. 3A).

342 Cell density in TAP(CO₂) cultures was more than three times higher compared to
343 photoautotrophic HSM cultures. However, a similar dry biomass at the end of cultivation
344 was observed for both, indicating that the reduced cell division rate was compensated for
345 by increased intracellular biomass accumulation in photoautotrophic HSM cultivations.

346 Accumulation of secreted *gLucLpIBP* in culture media correlated with relative culture cell
347 densities in each trial up to 72 hours of cultivation (Fig. 3A,B). Strictly photoautotrophic

348 production of *gLucLpIBP* was achieved to less than 2 mg L^{-1} in HSM, however, HiT
349 medium cultures accumulated $\sim 5\text{-}6 \text{ mg L}^{-1}$ *gLucLpIBP* without the addition of an organic
350 carbon source (Fig. 3B). Purely heterotrophic TAP cultivations produced $\sim 2 \text{ mg L}^{-1}$
351 *gLucLpIBP* from the 1 g L^{-1} acetate present in this medium (Fig. 3B). TAP(air) and
352 TAP(CO₂) photomixotrophic cultivations accumulated $\sim 10 \text{ mg L}^{-1}$ of this protein by 96 h
353 (Fig 3B), however, accumulation of *gLucLpIBP* in TAP(CO₂) cultivations occurred earlier
354 than TAP(air) cultivations, correlated with the higher cell densities achieved in these time
355 points (Fig. 3A, upper panel).

356 **3.3 Cultivation of UVcCA in flat panel and wave bag photobioreactor systems**

357 The potential for culture scale-up is of crucial importance for any biotechnological
358 production system. Therefore, after the establishment of optimal nutrition conditions in
359 400 mL small scale batch cultivations, two medium scale cultivation strategies were
360 compared in terms of culture growth parameters and secreted *gLucLpIBP* titres, a 10 L flat
361 panel bioreactor (Fig. 4A, left), designed to optimize light penetration into algal culture,
362 and a 10 L wave-bag system designed for the gentle cultivation of various cell types
363 (Fig. 4A, right), including Chinese Hamster Ovary (CHO) and insect cell culture (Baldi et
364 al. 2007; Ikonou et al. 2003). The flat-panel system has been described to produce high
365 biomass titres from microalgal strains due to optimized light penetrance into the culture
366 volume, a limiting factor for microalgal culture scale up (Posten 2009). The wave-bag
367 system represents a certified good manufacturing practice (cGMP) grade system which has
368 been adapted to tissue culture of another photosynthetic organism, the moss
369 *Physcomitrella patens* (Gitzinger et al. 2009), but was, to our knowledge, not yet applied
370 to eukaryotic microalgae.

371 Since the combination of TAP medium with 3% CO₂ gassing resulted in the best overall
372 culture performance as well as titres of secreted *gLucLpIBP* up to 10 mg L^{-1} (Fig. 3), these
373 conditions were chosen for the 10 L scale-up trials.

374 Growth parameters monitored from each cultivation are presented in Figure 4B.
375 Measurements from 400 mL photoheterotrophic batch test are included for reference.
376 Medium scale cultures were conducted for 6 days, and assessed for relative performance in
377 terms of cell density and dry biomass (Fig. 4B, upper and lower panels, respectively).

378 As expected, the flat panel system clearly outperformed the wave bag in terms of early
379 culture cell density, reaching $\sim 6.0 \pm 0.4 \times 10^7 \text{ cells mL}^{-1}$ within the first 48 h of cultivation.
380 However, these values declined after this point (Fig. 4B), indicating onset of cell death.

381 The wave bag system exhibited a steady increase in cell density throughout the trial,
382 reaching $\sim 4.0 \pm 0.7 \times 10^7$ cells mL⁻¹ at the end of cultivation period (Fig. 4B, upper panel).
383 Overall dry biomass of the flat panel system was up to 1.2 ± 0.06 g L⁻¹ which was similar to
384 the 400 mL culture at 96 hours (1.3 ± 0.10 g L⁻¹) and higher than the wave-bag system,
385 $\sim 0.9 \pm 0.10$ g L⁻¹ (Fig. 4B, lower panel).
386 In terms of algal biomass productivity, the flat panel system clearly outperformed the wave
387 bag system, even with a lower light intensity (Fig. 4B). Interestingly, the opposite was
388 observed for the amount of secreted *gLucLpIBP* in the culture medium. The wave bag
389 system accumulated the recombinant protein to ~ 12 mg L⁻¹ after 144 h of cultivation
390 (Fig. 4C). Therefore, in comparison to 400 mL cultures, in which ~ 7.5 - 10 mg L⁻¹ was
391 produced, the wave bag reached this protein titre within 96 h cultivation and even
392 surpassed this later (Fig. 4C). In contrast, the flat panel demonstrated only accumulation to
393 a maximum of ~ 2 mg L⁻¹ at 48 h cultivation, which was then even seemingly degraded
394 (Fig. 4C), coinciding with the decline in culture cell density (Fig. 4B). These results show
395 that despite slower biomass generation, the more gentle cultivation in the wave bag system
396 lead to overall higher recombinant protein production.

397 **3.4 IRI from algal produced *LpIBP* in a simplified ice-cream model solution**

398 The ice recrystallization inhibition activity of *gLucLpIBP* produced from UVcCA has been
399 demonstrated previously in total extracellular protein containing culture medium solutions
400 (Lauersen et al. 2013b). Since the primary commercial application for ice binding proteins
401 is proposed as cryopreservation and texturing of frozen foods (Griffith and Ewart 1995;
402 Hassas-Roudsari and Goff 2012), we intended to investigate if total concentrated
403 extracellular proteins (CEP) from UVcCA could be used to inhibit ice recrystallization in a
404 simplified ice cream model solution, consisting of 49% sucrose in water. As shown in
405 Figure 5A and quantified in Fig. 5B, *gLucLpIBP* containing CEP added to sucrose
406 solutions inhibited ice crystal growth as well as purified fish antifreeze protein, exhibiting
407 smaller crystal sizes for up to 168 hours, while the same concentration of extracellular
408 proteins from the parental strain (UVM4: WT) did not inhibit recrystallization and was
409 quantitatively comparable to sucrose solution used as negative control (Fig. 5B).

410

411 **4. Discussion**

412 Photosynthetic microalgae combine aspects of microbial growth, such as ease of
413 containment compared to transgenic plant systems and the capacity for simple,
414 photoautotrophic cultivation in inexpensive culture media. Therefore, these organisms
415 represent potentially sustainable hosts for recombinant bio-product generation (Wijffels et
416 al. 2013). Generally, bioprocesses seek to optimize for production of a single product,
417 often found within the cell, the harvesting of which is at the expense of the cell biomass, or
418 other valuable products found within. We previously demonstrated that, through secretion
419 of a target recombinant product into the culture medium, the product could be harvested
420 independently of the valuable algal biomass (Lauersen et al. 2013b). In this work, we
421 intended to optimize cultivation parameters that result in an enhanced production of an
422 industrially relevant secreted recombinant protein product concomitant with algal biomass
423 production.

424 Dry biomass generated in photoautotrophic cultivation matched mixotrophic levels at 96 h,
425 however, mixotrophic cultures had more than double cell density of all other cultures
426 (Fig. 3). The discrepancy is likely due to cell size variations in the different cultivation
427 media, as had been previously noted (Lauersen et al. 2013b). The differences in cell
428 density were reflected in the total *gLucLpIBP* secreted into culture media, where TAP(air)
429 or TAP(CO₂) cultivations again were the best performing (Fig. 3B). These results indicate
430 that although photoautotrophic production, which is the hallmark of the algal system, is
431 possible, optimization of cultivation media for secreted products is still necessary.

432 Heterotrophic cultivation is generally used for biotechnological systems based on bacteria
433 yeast, or fungi as production hosts (Schmidt 2004). Since the green alga *C. reinhardtii* also
434 offers the potential for strict heterotrophic growth, this option was tested in cultivations
435 including acetate as energy and carbon source in the dark. As demonstrated, this
436 cultivation strategy turned out to clearly be the worst of all options, given the low overall
437 biomass productivity and also low secreted *gLucLpIBP* observed from this cultivation style
438 (Fig. 3). In contrast, light-driven bioproduction was possible through photoautotrophic
439 cultivation of this strain in HiT medium, where strict photoautotrophic production of
440 secreted *gLucLpIBP* was possible up to ~5 mg L⁻¹ (Fig. 3B). It has to be mentioned though
441 that HiT medium contains 12 g L⁻¹ Tris, which is economically unfavourable to scale up.
442 Reduction of the Tris content even as little a 10 g L⁻¹ with this medium resulted in reduced
443 culture and secreted recombinant protein performance from modified HiT medium (not
444 shown).

445 Mixotrophic cultivation with TAP(CO₂) demonstrated higher productivities than all other
446 cultures as early as 24 h cultivation (Fig. 3A), likely due to the use of two carbon sources
447 for cell growth. Final cell densities for these cultivations were similar to those of both
448 mixotrophic TAP(air) and photoautotrophic HiT medium cultivations (Fig. 3), indicating
449 that use of two carbon sources has an additive effect on the productive capacity of this
450 algal system. The combination of acetate feeding with the photosynthetic capacity of *C.*
451 *reinhardtii* enhanced its photo-bioproduction capacity, resulting in the highest rates of
452 production observed in mixotrophic TAP(CO₂) and TAP(air) cultures. This mixotrophic
453 growth effect of boosting cell cultivation by simultaneous CO₂ supply and acetate feeding
454 has been recently shown in our laboratory as a mechanism regulated by the control of light
455 harvesting efficiency (Berger et al. 2014). Elevated CO₂ supply under mixotrophic
456 conditions causes the inhibition of translation repression of light harvesting proteins of
457 photosystem II, resulting in larger antennas and improved photosynthetic growth.

458 Previous experiments in small volume shake flasks of cultures expressing other secreted
459 RP targets, late logarithmic-early stationary phase was used as a harvesting point for these
460 cultures as no increase in product was observed after stationary phase was reached. This
461 was true for several fluorescent reporters in our laboratory, and used as the harvest point
462 for chromatography attempts with recombinant human erythropoietin secreted from *C.*
463 *reinhardtii* (Lauersen et al., 2015, Eichler-Stahlberg et al., 2009). We previously noted that
464 in certain conditions, secreted *gLucLpIBP* was less stable in high density bubbled cultures
465 after 72 h cultivation and it was proposed that repetitive batch cultures use a 72 h cycle, in
466 late logarithmic growth, to avoid product loss (Lauersen et al. 2013b). RP instability by 96
467 hours in turbid high-density culture may explain why TAP(air) cultivations reached titers
468 of *gLucLpIBP* comparable to TAP(CO₂) cultivations by 96 h.

469 The culture productivities observed from mixotrophic, TAP(CO₂), cultivations in small
470 scale indicated that this cultivation style should be used for scale-up to medium volume
471 systems. We chose to attempt cultivation of strain UV_cCA in a medium-volume flat panel
472 photobioreactor designed for optimal culture light penetrance for efficient photosynthetic
473 growth (depicted in Fig. 4A, left panels). This system indeed resulted in biomass
474 accumulation for strain UV_cCA similar to 400 mL cultivations, as well as a rapid increase
475 in cell density. However, in this culture, the rapid increase in cell density was not coupled
476 with high yields of the *gLucLpIBP*, which seemingly degraded after 48 h cultivation
477 (Fig. 4C). This was surprising, given in all previous cultivations higher cell densities
478 coincided with higher secreted RP yield (Fig. 3), however, suggested that culture turbidity

479 had a significant influence on secreted products in the culture medium. Indeed, the culture
480 within the flat panel reactor is exclusively mixed by gas flow aeration across the entire
481 base of the culture. It is possible that at these cell densities in this turbid environment,
482 some cell lysis occurs, resulting in protease release into culture medium. Although the flat
483 panel reactor allowed robust biomass productivities in medium scale-up, concomitant
484 *gLucLpIBP* accumulation within the medium in this cultivation set-up was significantly
485 hindered, indicating the flat panel system was not optimal for the proposed RP secretion-
486 production process.

487 For a secreted product, the balance between cell density and biomass productivity with the
488 stability and production of the secreted product must be considered. Given the issues for
489 *gLucLpIBP* production associated with high-density turbid cultivation in the flat panel
490 bioreactor system, we looked to a more gentle cultivation strategy employed for sensitive
491 cell cultures such as mammalian and insect cells, which had been previously used for
492 cGMP grade photosynthetic tissue culture and recombinant protein production from the
493 moss *P. patens* (Baldi et al. 2007; Gitzinger et al. 2009; Ikonomou et al. 2003).

494 Cultivation at the 10 L scale in the wave bag system, proved to be a viable option for
495 UVcCA cultivation and secreted *gLucLpIBP* production (Fig. 4). Biomass steadily
496 accumulated in this system to $\sim 0.9 \pm 0.10 \text{ g L}^{-1}$ (Fig. 4B), and secreted *gLucLpIBP*
497 accumulated to significant titres within 6 days of cultivation (Fig. 4C), surpassing that
498 observed after 96 hours cultivation in 400 mL (Fig. 3B). Turbidity in the wave bag system
499 was reduced, as gassing is injected to the bag on the culture surface, rather than bubbled
500 through the medium, which likely resulted in reduced shear stress to cells.

501 cGMP grade level cultivation in the wave bag system may be a valuable property for bio-
502 production as described for other human-use products (Decker and Reski 2012; Gitzinger
503 et al. 2009). Given the potential for the use of the *LpIBP* for frozen food IRI, a safe,
504 reliable cultivation strategy for production of this edible foodstuff is desirable (Griffith and
505 Ewart 1995). However, the inherent costs of these bag systems makes them unreasonable
506 for medium-value bulk food additive production, the list price for each bag can range from
507 €240-350, without additional filters or tubing (Sartorius Stedim Biotech, Germany).
508 Nevertheless, the concepts of surface gassing and gentle culture rocking to minimize shear
509 stress can be adapted to less expensive, food-grade plastic bag systems for microalgal
510 cultivation. In addition, we have previously demonstrated that several cycles of repetitive
511 batch cultivation of strain UVcCA is possible without inhibition of *gLucLpIBP* secretion

512 (Lauersen et al. 2013b). Therefore, bag systems could be re-used in a repetitive cultivation
513 style, to limit process overhead costs.

514 Ice binding proteins with IRI activity are proposed as additives to increase storage time of
515 frozen foods due to their ability to inhibit ice crystal growth at very low concentrations
516 (Feeney and Yeh 1998; Griffith and Ewart 1995). It has been determined that IBPs pose no
517 risk to human health, as these proteins are routinely consumed in the diets of people living
518 in northern climates (Crevel et al. 2002). A prominent example where these proteins may
519 be of use is as an additive to ice cream, in which recrystallization occurs within 24 hours of
520 storage, and is intensified in varying temperature storage (Donhowe and Hartel 1996a;
521 Donhowe and Hartel 1996b). Soluble protein extracts from cold-acclimated Winter Wheat,
522 a frost tolerant plant (Regand and Goff 2006b; Regand and Goff 2006a), as well as
523 different fish antifreeze proteins (Gaukel et al. 2014) have been shown to illicit IRI activity
524 in sucrose solutions. Given that the *LpIBP* can tolerate pasteurization (Pudney et al. 2003;
525 Sidebottom et al. 2000), and demonstrates a strong IRI as low as 0.055 μM (Yu et al.
526 2010), it is a prime candidate for this purpose. Additionally, microalgae are generally
527 regarded as safe for human consumption (GRAS) by the Food and Drug Administration of
528 the United States of America (Gantar and Svirčev 2008; Rasala and Mayfield 2014).
529 Therefore, we tested *LpIBP* secreted from *C. reinhardtii* UVcCA, which had demonstrated
530 IRI in pure media solutions previously (Lauersen et al. 2013b), in simplified ice-cream
531 model solutions (Fig. 5). In order to limit the downstream processing costs associated with
532 our algal product, total CEP from the algal culture was used, requiring only algal
533 separation and concentration prior to use (Lauersen et al. 2013b). Clear IRI activity was
534 detected in 49% sucrose after addition of total CEP samples from UVcCA cultures and
535 lasted for up to 7 days, when the experimental trials were ended (Fig. 5). In this work, we
536 did not study long term IRI, but since no signs for a decrease of IRI efficiency was
537 detectable after 7 days, it is likely that the IRI would be effective for a significantly longer
538 period of time. IRI did not occur for the equivalent CEP from the parental wild-type strain
539 or sucrose solutions alone (Fig. 5A,B), demonstrating the specificity of this effect from the
540 recombinant construct and indicating the possibility of using the CEP from transgenic
541 *C. reinhardtii* as a potential food additive.

542 Currently, a recombinant fish IBP is industrially produced in yeasts and used to texture
543 low-fat ice creams sold in the USA, Australia, and New Zealand (Penders 2011). AFP III
544 has been shown to be produced to $\sim 10\text{-}12 \text{ mg L}^{-1}$ in *Escherichia coli* (Chao et al. 1993),
545 and accumulates to $\sim 20 \text{ g L}^{-1}$ in fish blood (Fletcher et al. 1985). No data on this from

546 yeast is publically available, although RP titres from yeast systems can be up to several
547 grams per litre culture (Porro et al. 2005). *E. coli* recombinant expression of the *LpIBP* has
548 been reported up to $\sim 30 \text{ mg L}^{-1}$ (Middleton et al. 2009), however, processing to yield a
549 pure product requires several purification steps, including ice-affinity chromatography
550 which would be costly to scale-up, highlighting the value of minimal processing as with
551 CEP from GRAS algal culture. *LpIBP* exhibits IRI at dilutions as low as $0.055 \mu\text{M}$ (Yu et
552 al. 2010), for the 33-54 kDa *gLucLpIBP* species observed to be secreted from *C.*
553 *reinhardtii* (Lauersen et al. 2013a), this equates to concentrations between 1.8 mg L^{-1} to
554 3 mg L^{-1} protein required for the IRI effect.

555 Approximately 12 mg L^{-1} *gLucLpIBP* was produced in 144 h from UVcCA in the Wave
556 bag system, this titre equates to enough secreted product for up to $\sim 67 \text{ L}$ ice cream from a
557 single photomixotrophically cultivated 10 L algal culture bag. In order to make this
558 process cost effective, however, increased protein titres, process efficiency, perhaps
559 through serial cultivation of multiple 10 L bags, the use of other inexpensive cultivation
560 bags, and employing repetitive batch processes will be necessary.

561 **5. Conclusions**

562 Given the low media costs of algal cultivation, and the possibility of using the total
563 concentrated extracellular proteins without target RP purification, *C. reinhardtii* based
564 secretion of IBPs may represent a novel source for these food-texturing proteins. Scale-up
565 of algal systems presents many technical hurdles, and the data presented here indicate that
566 photobioreactors, which produce optimal culture biomass, may not necessarily be
567 productive for secreted RPs. Although most protein targets will require individualized
568 culture conditions, the secretion of *gLucLpIBP* presented here represents first insights into
569 the interplay of RP secretion behaviour and microalgal cultivation. The results of this work
570 suggest that traditionally secreted soluble recombinant products accumulate during cell
571 doubling, therefore, cultivation conditions which allow high-cell densities should be used
572 for production. In addition, sheer stress and turbidity should be reduced, in order to prevent
573 secreted RP degradation and loss. A balance between culture density and cultivation
574 parameters must exist to assist stable secreted RP in culture media. Photosynthetic
575 production capacity of *C. reinhardtii* is greater than its heterotrophic capacity, and through
576 addition of some organic carbon source, photo-bioproduction of a secreted RP was
577 enhanced. The wave bag system, which is cGMP grade, seems to provide a gentle
578 environment for both moderate cell growth and recombinant protein secretion, although

579 less expensive bag systems will need to be used to make this production style cost-
580 effective. It is likely that the reduced turbidity of this system was a major factor to allow
581 stable RP accumulation in culture medium. However, secreted recombinant protein titres
582 will need to be improved in order to make microalgae viable as an alternative for the
583 production of industrially relevant products for the food industry.
584

585 **6. Acknowledgements**

586 The authors would like to acknowledge the CLIB Graduate Cluster Industrial
587 Biotechnology (Federal Ministry of Science & Technology North Rhine Westphalia,
588 Germany (to K.J.L.)), The authors would like to express thanks to Prof. Dr. Ralph Bock for
589 strain UVM4. Thanks as well to Isabell Kaluza and Michael Grundmann for assistance in
590 photoautotrophic media pre-screening

591 **7. Conflict of Interest**

592 The authors declare that they have no conflict of interest.

593 **8. References**

- 594 Baldi L., Hacker D., Adam M., Wurm F., 2007. Recombinant protein production by large-
595 scale transient gene expression in mammalian cells: state of the art and future
596 perspectives. *Biotechnol Lett.* 29(5), 677–684.
- 597 Bateman J.M., Purton S., 2000. Tools for chloroplast transformation in *Chlamydomonas*:
598 expression vectors and a new dominant selectable marker. *Mol Genet Genomics.* 263,
599 404–410.
- 600 Berger H., Blifernez-Klassen O., Ballottari M., Bassi R., Wobbe L., Kruse O., 2014.
601 Integration of carbon assimilation modes with photosynthetic light capture in the
602 green alga *Chlamydomonas reinhardtii*. *Mol Plant.* 7, 1545–1559.
- 603 Chao H., Davies P.L., Sykes B.D., Sönnichsen F.D., 1993. Use of proline mutants to help
604 solve the NMR solution structure of type III antifreeze protein. *Protein Sci.* 2(9),
605 1411–28.
- 606 Crevel R.W.R., Fedyk J.K., Spurgeon M.J., 2002. Antifreeze proteins: characteristics,
607 occurrence and human exposure. *Food Chem Toxicol.* 40(7), 899–903.
- 608 Eichler-Stahlberg, A., Weisheit, W., Ruecker, O. Heitzer, M., 2009. Strategies to facilitate
609 transgene expression in *Chlamydomonas reinhardtii*. *Planta* 229, 873–883.
- 610 Decker E.L., Reski R., 2012. Glycoprotein production in moss bioreactors. *Plant Cell Rep.*
611 31(3), 453–460.
- 612 Donhowe D.P., Hartel R.W., 1996a. Recrystallization of ice in ice cream during controlled
613 accelerated storage. *Int Dairy J.* 6(11-12), 1191–1208.
- 614 Donhowe D.P., Hartel R.W., 1996b. Recrystallization of ice during bulk storage of ice
615 cream. *Int Dairy J.* 6(11-12), 1209–1221.
- 616 Feeney R.E., Yeh Y., 1998. Antifreeze proteins: Current status and possible food uses.
617 *Trends Food Sci Technol.* 9(3), 102–106.
- 618 Fletcher G.L., Hew C.L., Li X., Haya K., Kao M.H., 1985. Year-round presence of high
619 levels of plasma antifreeze peptides in a temperate fish, ocean pout (*Macrozoarces*
620 *americanus*). *Can J Zool.* 63(3), 488–493.
- 621 Franklin S.E., Mayfield S.P., 2004. Prospects for molecular farming in the green alga
622 *Chlamydomonas reinhardtii*. *Curr Opin Plant Biol.* 7(2), 159–165.
- 623 Gantar M., Svirčev Z., 2008. Microalgae and Cyanobacteria: Food for Thought. *J Phycol.*
624 44(2), 260–268.
- 625 Gaukel V., Leiter A., Spieß W.E.L., 2014. Synergism of different fish antifreeze proteins
626 and hydrocolloids on recrystallization inhibition of ice in sucrose solutions. *J Food*
627 *Eng.* 141, 44–50.
- 628 Gimpel J.A., Hyun J.S., Schoepp N.G., Mayfield S.P., 2014. Production of recombinant
629 proteins in microalgae at pilot greenhouse scale. *Biotechnol Bioeng.* 112(2), 339–345.
- 630 Gitzinger M., Parsons J., Reski R., Fussenegger M., 2009. Functional cross-kingdom
631 conservation of mammalian and moss (*Physcomitrella patens*) transcription,
632 translation and secretion machineries. *Plant Biotechnol J.* 7(1), 73–86.
- 633 Gorman D.S., Levine R.P., 1965. Cytochrome f and plastocyanin: their sequence in the
634 photosynthetic electron transport chain of *Chlamydomonas reinhardtii*. *Proc Natl Acad*
635 *Sci.* 54(6), 1665–1669.
- 636 Griffith M., Ewart K. V., 1995. Antifreeze proteins and their potential use in frozen foods.
637 *Biotechnol Adv.* 13(3), 375–402.
- 638 Hassas-Roudsari M., Goff H.D., 2012. Ice structuring proteins from plants: Mechanism of
639 action and food application. *Food Res Int.* 46(1), 425–436.
- 640 Hew C.L., Slaughter D., Joshi S.B., Fletcher G.L., Ananthanarayanan V.S., 1984.
641 Antifreeze polypeptides from the Newfoundland ocean pout, *Macrozoarces*

642 *americanus*: presence of multiple and compositionally diverse components. J Comp
643 Physiol B. 155, 81–88.

644 Hew C.L., Wang N.C., Joshi S., Fletcher G.L., Scott G.K., Hayes P.H., Buettner B., Davies
645 P.L., 1988. Multiple genes provide the basis for antifreeze protein diversity and
646 dosage in the ocean pout, *Macrozoarces americanus*. J Biol Chem. 263(24), 12049–
647 12055.

648 Ikonomidou L., Schneider Y.J., Agathos S.N., 2003. Insect cell culture for industrial
649 production of recombinant proteins. Appl Microbiol Biotechnol. 62(1), 1–20.

650 Kindle K.L., 1990. High-frequency nuclear transformation of *Chlamydomonas reinhardtii*.
651 Proc Natl Acad Sci USA. 87(3), 1228–1232.

652 Lauersen K.J., Berger H., Mussgnug J.H., Kruse O., 2013a. Efficient recombinant protein
653 production and secretion from nuclear transgenes in *Chlamydomonas reinhardtii*. J
654 Biotechnol. 167(2), 101–110.

655 Lauersen K.J., Brown A., Middleton A., Davies P.L., Walker V.K., 2011. Expression and
656 characterization of an antifreeze protein from the perennial rye grass, *Lolium perenne*.
657 Cryobiology. 62(3), 194–201.

658 Lauersen K.J., Kruse O., Mussgnug J.H., 2015. Targeted expression of nuclear transgenes
659 in *Chlamydomonas reinhardtii* with a versatile, modular vector toolkit. Appl
660 Microbiol Biotechnol. doi: 10.1007/s00253-014-6354-7

661 Lauersen K.J., Vanderveer T.L., Berger H., Kaluza I., Mussgnug J.H., Walker V.K., Kruse
662 O., 2013b. Ice recrystallization inhibition mediated by a nuclear-expressed and -
663 secreted recombinant ice-binding protein in the microalga *Chlamydomonas*
664 *reinhardtii*. Appl Microbiol Biotechnol. 97(22), 9763–9772.

665 Mayfield S.P., Manuell A.L., Chen S., Wu J., Tran M., Siefker D., Muto M., Marin-
666 Navarro J., 2007. *Chlamydomonas reinhardtii* chloroplasts as protein factories. Curr
667 Opin Biotechnol. 18(2), 126–133.

668 Middleton A.J., Brown A.M., Davies P.L., Walker V.K., 2009. Identification of the ice-
669 binding face of a plant antifreeze protein. FEBS Lett. 583(4), 815–819.

670 Neupert J., Karcher D., Bock R., 2009. Generation of *Chlamydomonas* strains that
671 efficiently express nuclear transgenes. Plant J. 57(6), 1140–1150.

672 Penders B., 2011. Cool and safe: multiplicity in safe innovation at unilever. Bull Sci
673 Technol Soc. 31(6), 472–481.

674 Porro D., Sauer M., Branduardi P., Mattanovich D., 2005. Recombinant protein production
675 in yeasts. Mol Biotechnol. 31(3), 245–259.

676 Posten C., 2009. Design principles of photo-bioreactors for cultivation of microalgae. Eng
677 Life Sci. 9(3), 165–177.

678 Pudney P.D.A., Buckley S.L., Sidebottom C.M., Twigg S.N., Sevilla M.P., Holt C.B.,
679 Roper D., Telford J.H., McArthur A.J., Lillford P.J., 2003. The physico-chemical
680 characterization of a boiling stable antifreeze protein from a perennial grass (*Lolium*
681 *perenne*). Arch Biochem Biophys. 410(2), 238–245.

682 Rasala B.A., Barrera D.J., Ng J., Plucinak T.M., Rosenberg J.N., Weeks D.P., Oyler G.A.,
683 Peterson T.C., Haerizadeh F., Mayfield S.P., 2013. Expanding the spectral palette of
684 fluorescent proteins for the green microalga *Chlamydomonas reinhardtii*. Plant J.
685 74(4), 545–56.

686 Rasala B.A., Lee P.A., Shen Z., Briggs S.P., Mendez M., Mayfield S.P., 2012. Robust
687 expression and secretion of Xylanase1 in *Chlamydomonas reinhardtii* by fusion to a
688 selection gene and processing with the FMDV 2A peptide. PLoS One. 7(8), e43349.

689 Rasala B.A., Mayfield S.P., 2014. Photosynthetic biomanufacturing in green algae;
690 production of recombinant proteins for industrial, nutritional, and medical uses.
691 Photosynth Res. doi: 10.1007/s11120-014-9994-7

692 Regand A., Goff H.D., 2006a. Ice recrystallization inhibition in ice cream as affected by
693 ice structuring proteins from winter wheat grass. *J Dairy Sci.* 89(1), 49–57.
694 Regand A., Goff H.D., 2006b. Freezing and ice recrystallization properties of sucrose
695 solutions containing ice structuring proteins from cold-acclimated Winter Wheat grass
696 extract. *J Food Sci.* 70(9), E552–E556.
697 Remacle C., Cardol P., Coosemans N., Gaisne M., Bonnefoy N., 2006. High-efficiency
698 biolistic transformation of *Chlamydomonas* mitochondria can be used to insert
699 mutations in complex I genes. *Proc Natl Acad Sci U S A.* 103(12), 4771–4776.
700 Rochaix J.D., 1995. *Chlamydomonas reinhardtii* as the photosynthetic yeast. *Annu Rev*
701 *Genet.* 29, 209–230.
702 Rosales-Mendoza S., Paz-Maldonado L.M.T., Soria-Guerra R.E., 2012. *Chlamydomonas*
703 *reinhardtii*; as a viable platform for the production of recombinant proteins: current
704 status and perspectives. *Plant Cell Rep.* 31(3), 479–494.
705 Schmidt F.R., 2004. Recombinant expression systems in the pharmaceutical industry. *Appl*
706 *Microbiol Biotechnol.* 65(4), 363–372.
707 Sidebottom C., Buckley S., Pudney P., Twigg S., Jarman C., Holt C., Telford J., McArthur
708 A., Worrall D., Hubbard R., Lillford P., 2000. Heat-stable antifreeze protein from
709 grass. *Nature.* 406(6793), 256.
710 Sueoka N., 1960. Mitotic replication of deoxyribonucleic acid in *Chlamydomonas*
711 *reinhardtii*. *Proc Natl Acad Sci.* 46, 83–91.
712 Wijffels R.H., Kruse O., Hellingwerf K.J., 2013. Potential of industrial biotechnology with
713 cyanobacteria and eukaryotic microalgae. *Curr Opin Biotechnol.* 24(3), 405–413.
714 Yu S.O., Brown A., Middleton A.J., Tomczak M.M., Walker V.K., Davies P.L., 2010. Ice
715 restructuring inhibition activities in antifreeze proteins with distinct differences in
716 thermal hysteresis. *Cryobiology.* 61(3), 327–334.
717
718

719 9. Figures

720

721 **Fig. 1** Addition of the *LpIBP* to the C-terminus of *gLuc* results in increased recombinant
722 protein secretion. Presented are average bioluminescence signals of pre-stationary phase
723 TAP grown cultures for four strains isolated from transformant populations generated with
724 either *pOpt_cCA_gLuc_Paro* or *pOpt_cCA_gLuc_LpIBP_Paro* vectors (A).
725 Bioluminescence signals from TAP grown cultures were normalized to cell density for
726 four strains selected as the highest producers amongst 480 randomly picked colonies
727 generated from either vector in triplicate transformations (B). Error bars indicate standard
728 deviation. **H**: heat shock protein 70A promoter; **R**: ribulose biphosphate
729 carboxylase/oxygenase small subunit 2 (RBCS2) promoter; **i1/2** intron 1/2 of
730 *C. reinhardtii* RBCS2; **cCA** carbonic anhydrase secretion signal; **3'** RBCS2 3'
731 untranslated region.

732

733 **Fig. 2** Precondition growth and secreted recombinant protein expression analysis of
734 *UVcCA* in TAP medium. **A,B** 1 L shake, baffled shake, or stirred TAP medium cultures
735 were used to determine appropriate cultivation styles for *gLucLpIBP* production. Culture
736 cell density (A) and productivities of *gLucLpIBP* for each style, analyzed by dot blot of
737 1 μ l culture medium with α -*gLuc* antibody (B), are presented over 144 h cultivation.

738

739 **Fig. 3** Analysis of strain *UVcCA* in 3 media and different cultivation conditions at the
740 400 mL scale with stir mixing and gas bubbling. TAP media, with 1 g L⁻¹ acetate, was used
741 for cultivation in three different conditions, with addition of 3% CO₂, with only air, or in
742 the dark with air. HSM and HiT media were used for strictly photoautotrophic cultivations
743 with only 3% CO₂ as a carbon source. **A** Cell density and dry biomass (upper and lower
744 panels, respectively) were recorded and secreted *gLucLpIBP* was quantified from daily
745 culture samples by dot-blot against the *gLuc* portion of the fusion protein (B).
746 Recombinant *gLuc* produced by secretion from in *K. lactis* was used as a standard.

747

748 **Fig. 4** *UVcCA* cultivation in medium volume scale-up. **A** Left panel, the 10 L flat panel
749 reactor at 96 hours of cultivation, right panels depict the rocking 10 L wave bag reactor at
750 96 hours cultivation. **B** Culture growth parameters in 10 L flat panel and 10 L wave bag
751 bioreactors. Values recorded from 400 mL TAP with 3% CO₂ cultivation are added for
752 comparison. Cell density and dry biomass (upper and lower graphs, respectively) are

753 presented. **C** Accumulated *gLucLpIBP* in culture media from each system. Samples from
754 400 mL TAP 3% CO₂ cultures, 10 L flat panel, and 10 L wave bag are compared in dot
755 blot of 1 µl culture media with an anti-*gLuc* antibody. WT, indicates culture medium from
756 a 10 L cultivation of parental strain at 96 h and a 10X concentration of this protein extract
757 to demonstrate the antibody specificity for *gLuc* and minimal background from native *C.*
758 *reinhardtii* secreted proteins. The standard dilution series (right) was produced using
759 recombinant *gLuc* from *K. lactis*.

760

761 **Fig. 5** Demonstration of ice recrystallization inhibition activity using concentrated UVcCA
762 culture supernatant in simplified ice cream model solutions. **A** Recrystallization occurs
763 readily in 49% sucrose solution containing concentrated parental strain (WT) extracellular
764 proteins while secreted *gLucLpIBP* from UVcCA or a purified fish antifreeze protein (AFP
765 type III, from *M. americanus*) demonstrate effective ice recrystallization inhibition
766 activities up to 168 h. Bar represents 100 µm. **B** Quantitative measurements of mean
767 crystal sized in the four tested solutions including sucrose control.

768

769

770 **10. Supplemental Data**771 **Table S1 In house High-Tris medium**

1. First prepare 100mM Tris (60.57 g in 3L), then pH to 7.3 (with an abundance of 37% HCl)
2. Then add stock solutions as follows:

Solution	mL of stock solution used for 5L medium	mL of stock solution used for 1L medium
NH ₄ NO ₃	50	10
CaCl ₂ .2H ₂ O	10	2
MgSO ₄ .7H ₂ O	100	20
KH ₂ PO ₄	10	2
FeSO ₄ .7H ₂ O	5	1
CuSO ₄ .5H ₂ O	5	1
MnCl ₂ .4H ₂ O	5	1
ZnSO ₄ .7H ₂ O	5	1
H ₃ BO ₃	5	1
(NH ₄) ₆ Mo ₇ O ₂₄ .4H ₂ O	5	1
CoCl ₂ .6H ₂ O	5	1
Na ₂ SeO ₃	5	1
Na ₂ SiO ₃ .5H ₂ O	5	1
EDTA Disodium Salt, pH8	5	1

Fill to 5 L with ddH₂O

To prepare 500 mL of each stock solution

Stock solutions	g 500 mL⁻¹	Molecular weight (g mol⁻¹)	Concentration factor	conc. in culture medium (mM)
NH ₄ NO ₃	60.03	80.04	100	15
CaCl ₂ .2H ₂ O	31.24	147.01	1000	0.425
MgSO ₄ .7H ₂ O	9.24	246.48	100	0.750
KH ₂ PO ₄	68.05	136.09	100	10
FeSO ₄ .7H ₂ O	0.14	278.01	1000	0.001
CuSO ₄ .5H ₂ O	0.80	249.68	1000	0.0064
MnCl ₂ .4H ₂ O	2.55	197.90	1000	0.0258
ZnSO ₄ .7H ₂ O	11.07	287.56	1000	0.077
H ₃ BO ₃	5.69	61.83	1000	0.184
(NH ₄) ₆ Mo ₇ O ₂₄ .4H ₂ O	0.55	1235.87	1000	0.0009
CoCl ₂ .6H ₂ O	0.80	237.93	1000	0.0067
Na ₂ SeO ₃	0.01	172.94	1000	0.0001
Na ₂ SiO ₃ .5H ₂ O	28.96	212.14	1000	0.273
EDTA Disodium Salt, pH8	100.00	372.24	1000	0.5373

772

Figure 1
[Click here to download high resolution image](#)

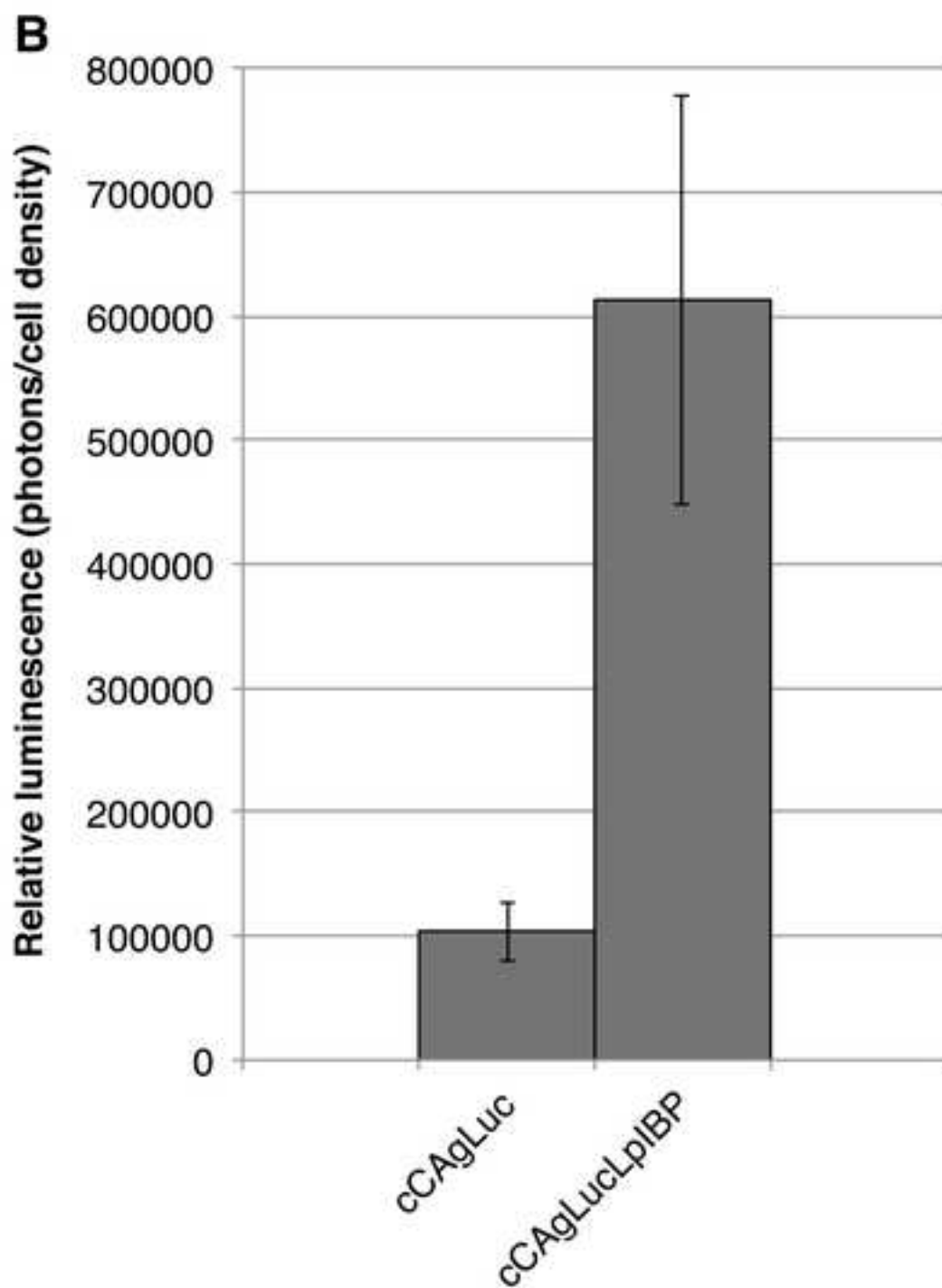
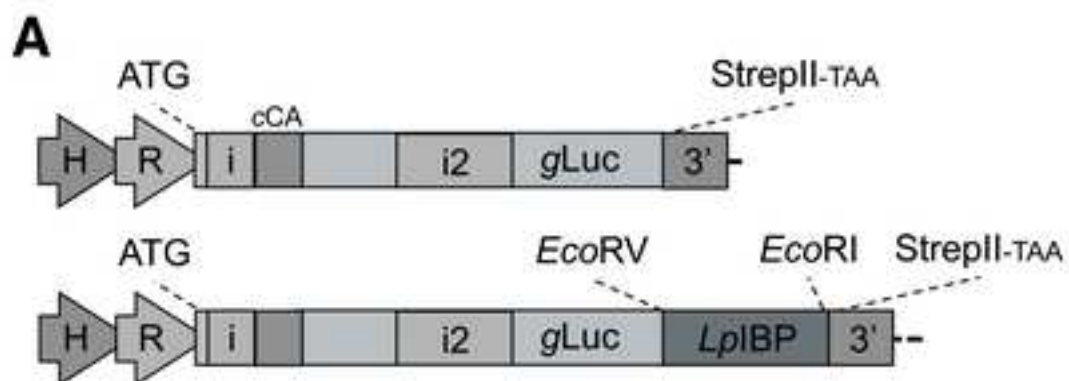


Figure 2
[Click here to download high resolution image](#)

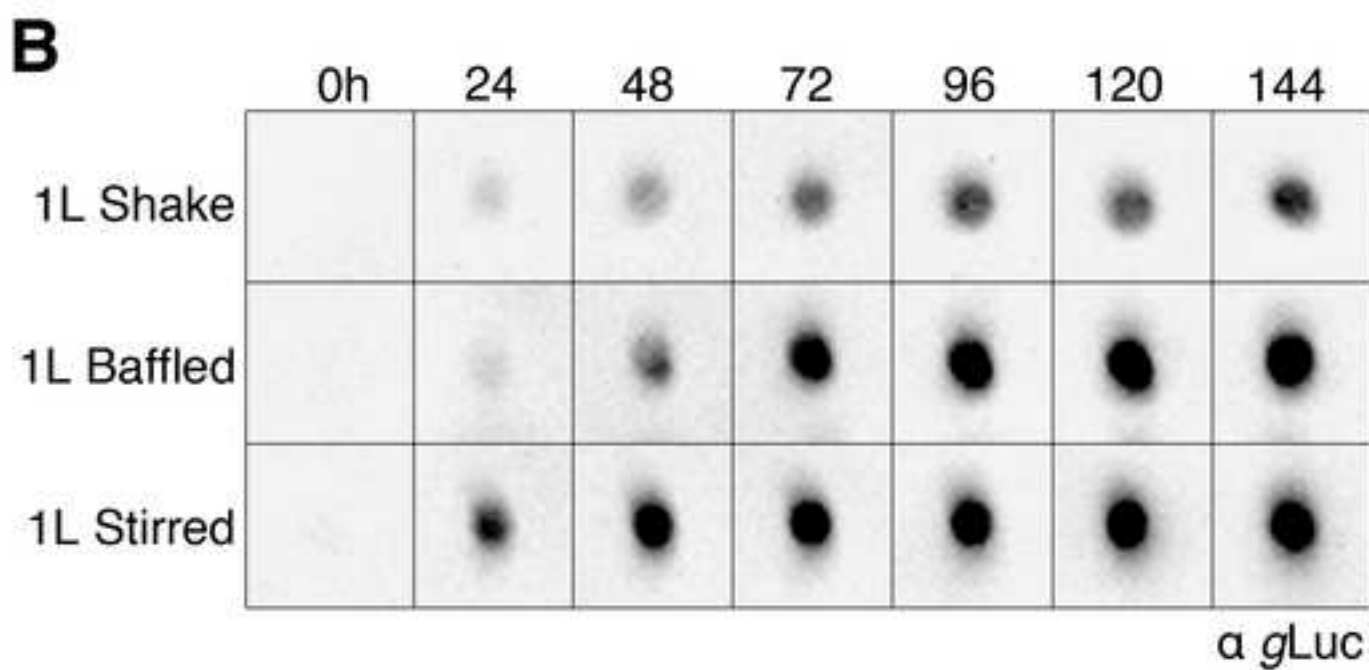
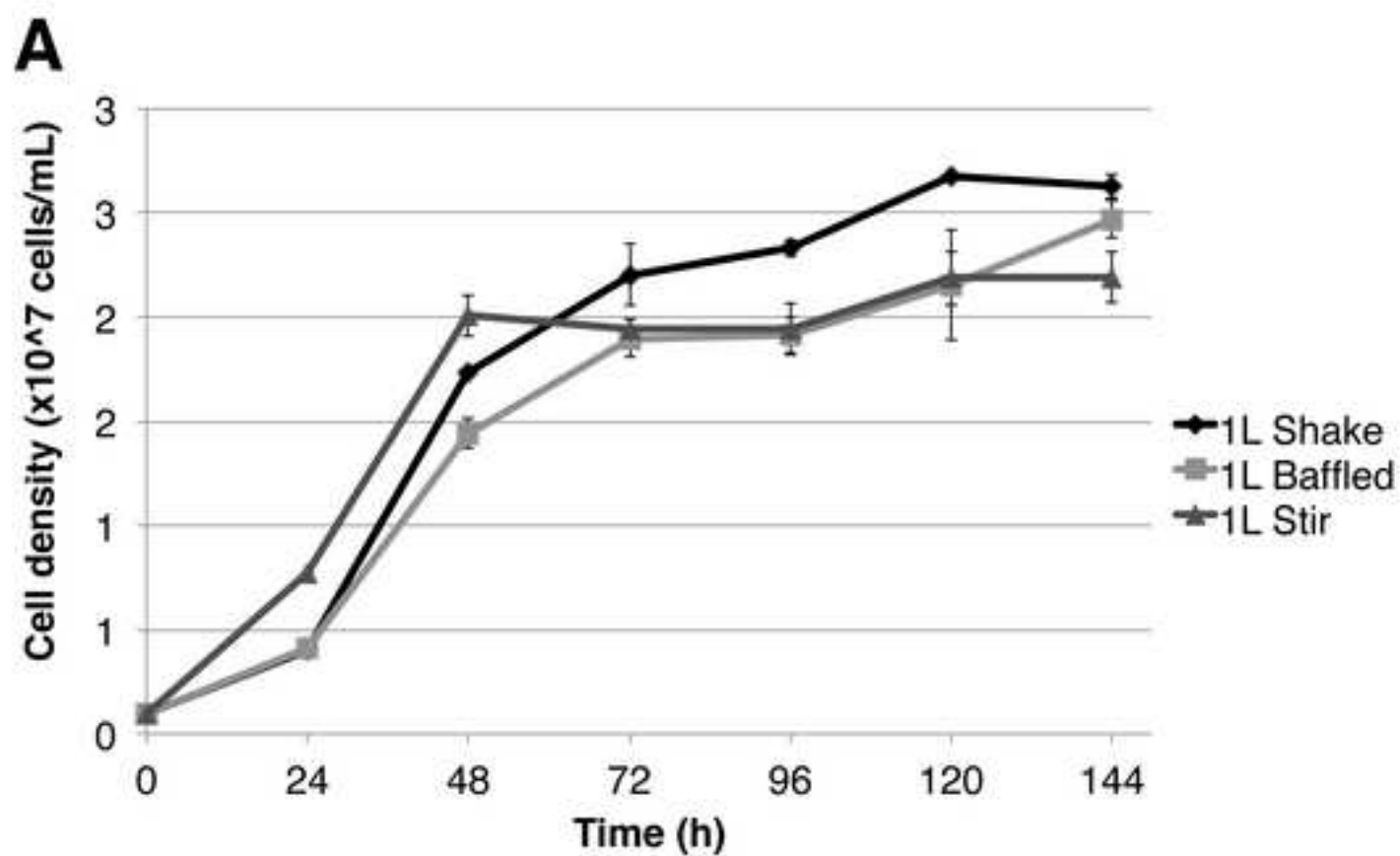


Figure 3

[Click here to download high resolution image](#)

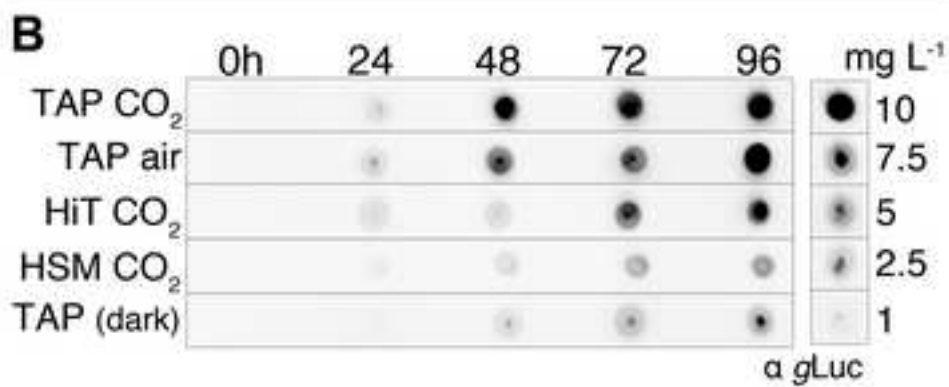
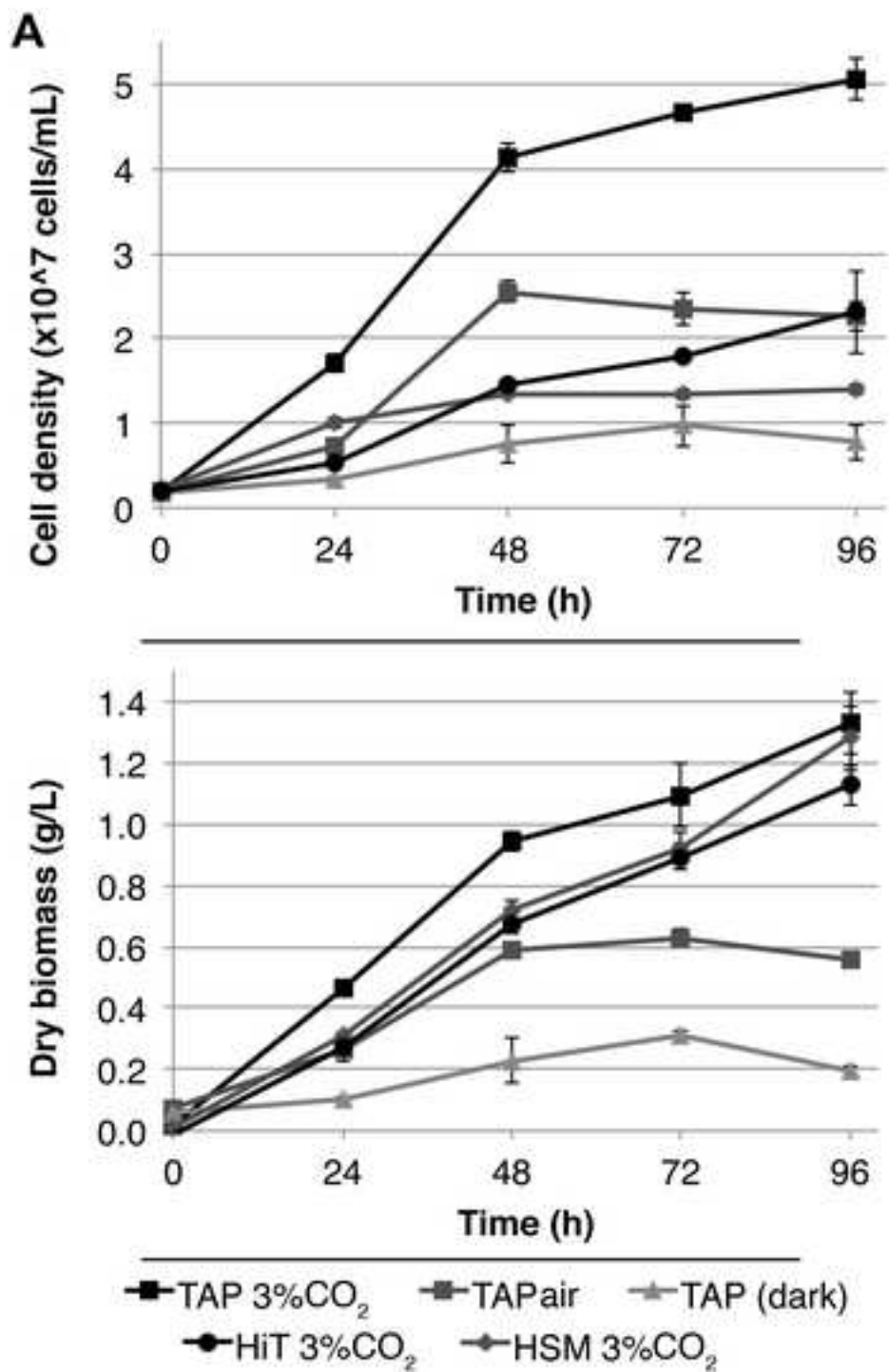


Figure 4

[Click here to download high resolution image](#)

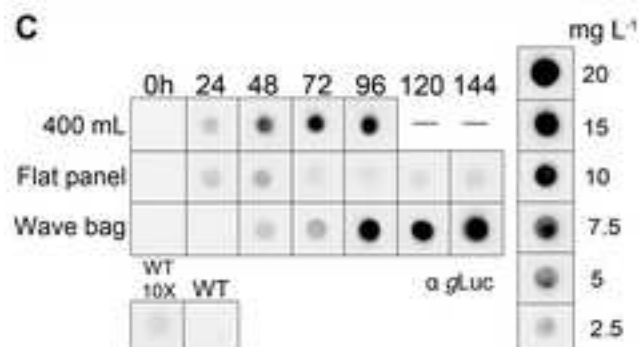
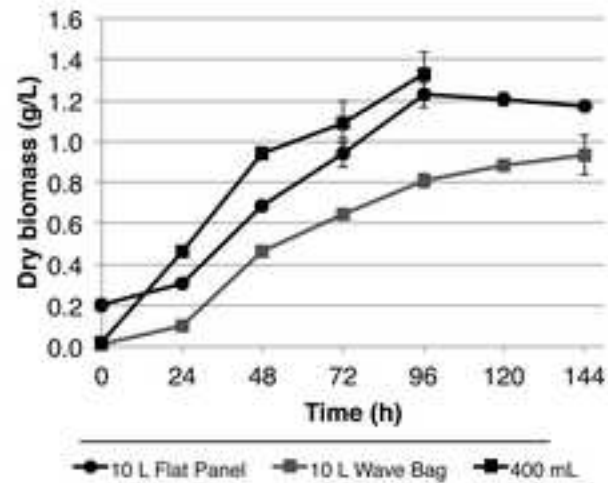
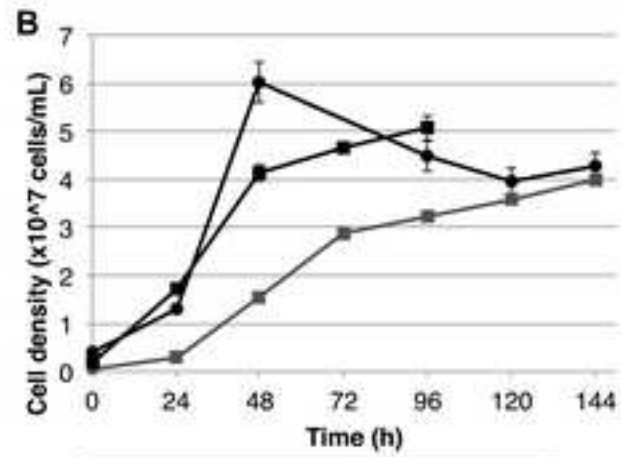


Figure 5

[Click here to download high resolution image](#)

